Review

Recent Trends in Minimization of Torque Ripples in Switched Reluctance Machine

Deepa Nidanakavi[a], Dr. K.Krishnaveni[b] and Dr. G. Mallesham[c]

[a]Department of Electrical and Electronics Engineering, Osmania University, Hyderabad, India, deepa-nidanakavi@gmail.com.
[b]Department of Electrical and Electronics Engineering, CBIT, Hyderabad, India. krishna-veni2k12.rvr@gmail.com.
[c]Department of Electrical and Electronics Engineering, Osmania University, Hyderabad, India.
* Correspondence: gm.eed.cs@gmail.com.

Abstract: Increased definite power, reduced cost, and dynamic construction are the important features required by electric motors for various applications. One such motor accommodating all the requisites mentioned above is Switched reluctance. Applications pertaining to small, commercial, and EV find Switched reluctance machine as a developing competitor to the conventional induction and permanent magnet motors. Though SRMS contribute a considerable number of advantages over induction motors and permanent magnet motors, the primary disadvantages pertaining to SRMs are the torque ripple, especially at high-speed operation, and the resulting acoustic noise. These disadvantages may not always be detrimental to the systems in entirely all cases, but depending on the application to be employed, torque ripple and acoustic noise form are detrimental to the system. This paper reviews the technology status and recent trends in the minimization of torque ripples switched reluctance machines.

Keywords: switched reluctance motor; direct instantaneous torque sharing function; rotor angle

1. INTRODUCTION

A switched reluctance motor (SRM), has a robust mechanical design and is modest structure and is prominent for it. The construction of the motor consists of a stator and a steel laminated rotor. The windings are of concentrated ty 23 around the stator pole. This simplicity in its construction makes it an attractive choice for a varied range of applications from domestic appliances to automotive along with heavy industrial applications. [1-3]. Permanent magnets are expensive and thus with their absence, SRM is emerging to be a promising alternative to permanent magnet machines. Despite the features of SRMS with inherent ruggedness, simplicity, and extensive development, variable-speed applications are sluggish in amenable SRMs as found from the studies over the past two decades [4].

When put into servo-type applications especially, the control requirements to be met for the SRM substantiate to be deceptively complicated. These disadvantages may not always be detrimental to the systems in entirely all cases, but depending on the application to be employed, torque ripple and a resultant acoustic noise form are detrimental to the system. In comparison with other AC machines that have rounded cores, SRM produces a relatively high torque ripple inherently owing to its structure being a doubly salient, singly excited machine and non-linear magnetic characteristics due to the non-linear inductance profile of SRM [5,6]. The torque ripple bears out to be intolerable in servo or servo-type systems. In these systems, the presence of torque ripple is sorely felt by the user or it may be emulated on the load precariously. And as watch to overcome this issue significant progress with conforming success has been made in the past decade and is now proven to be superior to the drives constructed in the primordial phases of development which performed notably noisy with large torque ripples [7]. The applications of SRM can be expanded with the reduction of torque ripples. This can be achieved primarily by employing two approaches. One method is by improving the machine

Preprints (www.preprints.org) | NOT PEER-REVIEWED | Posted: 7 December 2022 doi:10.20944/preprints202212.0119.v1

design with regard to the magnetic design, and the other method is the implementation of sophisticated electronic control techniques. The pulsations in the torque can be curtailed by changing the pole structures of the stator and rotor. But these changes come at an expense of motor outputs that are specific to SRM. In the electronic controller approach, optimization of control parameters such as the current levels, supply voltages, and change in the turn-on and turn-off angles, which affect the generated electromagnetic torque in SRM which in turn depends on the excitation angle corresponding to the rotor position. The approach of electronic control in minimizing torque ripple may reduce the average torque output. This is due to the non-utilization of motor capabilities to the full extent at all power levels [8] Some other methods also include the implementation of sense winding to sense the phase, the Finite Element Method (FEM).

This paper presents the review of torque ripple minimization techniques used SRM. The paper is formatted in the following lineup: Section II presents the elemental details of SRM such as the mechanical structure of SRM, and the approaches torque production. Section III discusses the operating conditions leading to torque ripple. In Section IV, realization of torque ripple minimization through machine design considerations and control strategy improvement are reviewed.

2. Switched Reluctance Motor Structure

The structure of SRM consists of three parts, stator, rotor, and winding. The most common traditional SRMs with distinctive stator and rotor pole ratios are illustrated in Figure 1 [19]. It is seen that the Magnetic flux in3nes to have a minimum reluctance. And this tendency is the reason for the production of the electromagnetic torque in the SRM. Once the rotor pole is aligned to the stator pole, the maximum inductance of the exciting phase is obtained.

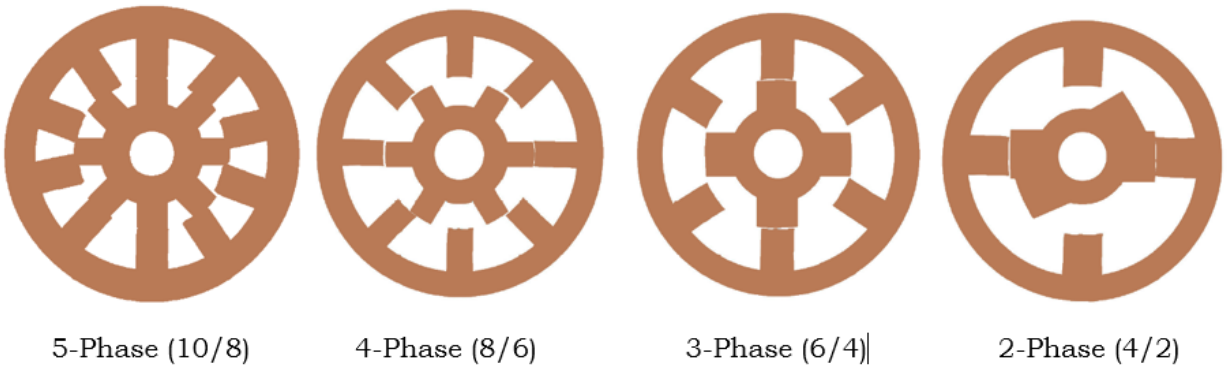

Fig 1. SRM Structure

The Equation for the instantaneous voltage between the terminals of a single phase can be expressed as

$$V = iR + \frac{d\phi}{dt}$$

where V is the instantaneous voltage on each phase, i is the phase current, R is the resistance of a phase, ϕ is the flux linkage, and t is the time. The changes in the flux linkage with the rotor position and phase current value

$$V = iR + \frac{\partial\phi}{\partial I}\frac{di}{dt} + \frac{\partial\phi}{\partial\theta}\frac{d\theta}{dt}$$

$$= iR + L(\theta, i)\frac{di}{dt} + E(\theta, i)\frac{d\theta}{dt}$$

where θ is the rotor position, $E(\theta, i)$ is the back electromotive force (EMF), and $L(\theta, i)$ is the instantaneous inductance.

The mechanical equation of the SRM is assumed as [10]

Preprints (www.preprints.org) | NOT PEER-REVIEWED | Posted: 7 December 2022 doi:10.20944/preprints202212.0119.v1

$$J\frac{d\omega}{dt} = T_e - T_L - T_0$$

$$\omega = \frac{d\theta}{dt}$$

Where J is the inertia due to the rotation, ω is the rotational angular speed, T_e is the electromagnetic torque, T_L is the load torque, T_0 is the additional torque encompassing frictiona torque, air resistance torque, etc. In [11] the authors have presented a design and enhanced a 12/8 pole SRM for EVs and hybrid EVs (HEV). With this optimization method, the torque ripple is found to be curtailed by 10.2%, and the average torque is escalated by 2.4%. These values are expressed in comparison to a typical benchmark design. In [11] the authors thus concluded that the initial torque can be increased in the most effective way by increasing the rotor diameter.

2.1. Winding Configurations

The winding configurations govern the performance of SRMS. In Figure 2, a representation of the winding configurations for different reluctance motors is given [12-14]. Winding the phase coil on one pole of the stator by placing only one coil in each slot is one configuration known as single-layer concentrated (SLC) winding. The other configuration is the single-layer mutually coupled (SLMC) windings and the SLC windings with a distinctive winding direction. The change caused in the self and mutual inductances produces the torque in SRM for the SLMC windings. And the change in the self-inductances produces the torque in the conventional SRM for the SLC winding [15-16]. In another configuration of double layer mutually coupled (DLMC) winding every slot is shared by two coils. The same is practiced in the double layer concentrated (DLC) winding. Figure 3 shows the representation of DLMC and DLC configurations. And another winding configuration is that of fully pitched (FP) winding is represented in Figure 4. Here, a distributed winding SRM called mutually coupled SRM (MCSRM) is adopted. For some combinations of the pole and stator phase, SLMC and DLC may not be viable. One of the reasons for this is the unbalanced winding.

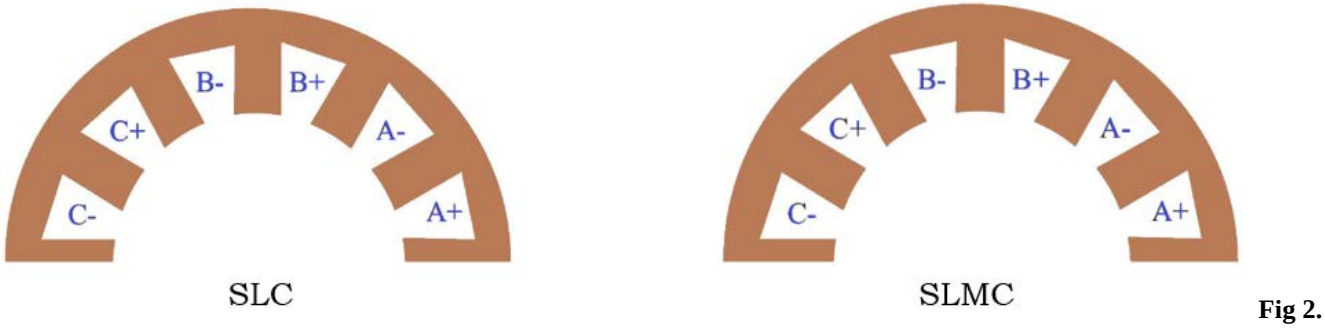

Fig 2. single-layer concentrated (SLC) winding and single-layer mutually coupled (SLMC) windings

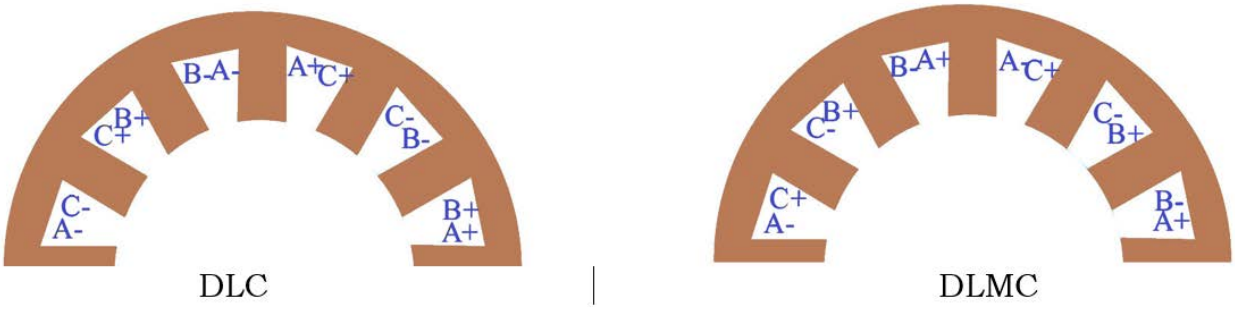

Preprints (www.preprints.org) | NOT PEER-REVIEWED | Posted: 7 December 2022 doi:10.20944/preprints202212.0119.v1

Fig 3. double-layer concentrated (DLC) winding and double-layer mutually coupled (DLMC) windings

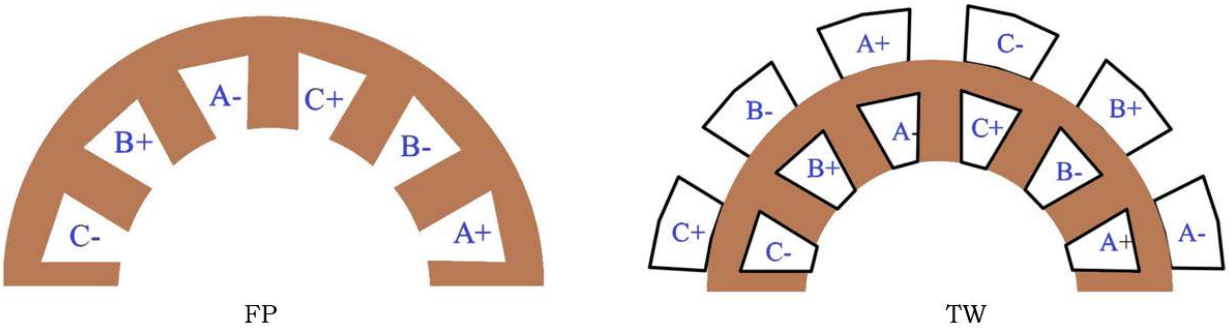

Fig 4. fully-pitched (FP) and toroidal winding

An unconventional SRM with multiple isolated flux (MIFPS) has been proposed to attain lesser eddy current and hysteresis losses [17-18]. This configuration is characterized by higher torque density than that of a traditional SRM. The toroidal winding configuration is also depicted in Fig. 4. It is in SRM with 12/10 MIFP. The toroidal winding improves the heat transfer which proves to be an advantage so that the stator and rotor teeth can be designed to be wide. This design improves the fill factor and thus results in the reduction of the acoustic noise at low speeds, the MCSRM configuration accomplishes higher torque performance per ampere at low speeds. Also, at higher speeds, the back-EMF voltage is higher in MCSRM [19-20]. When the winding configurations described above are compared, torque ripple is lower along with higher average torque is found to be achieved in the SRM with FP winding than with the SRMS using the configurations of DLC or DLMC, SLC, SLMC windings [22]. In [23], a model for toroidal winding SRM (TWSRM) was proposed. The design configuration in TWSRM is provided with an additional winding space enabling the advantages of mutual coupling excitation to be maintained. The TWSRM when compared to the MCSRM produces a more concentrated magnetomotive force (MMF). Also, it is more susceptible according to saturation. Among all the winding configurations of the SRM, the highest torque in the high-speed region is achieved in the MCSRM and the highest torque in the low-speed region is produced in the TWSRM [24].

2.2. Torque Calculation in Switched Reluctance Motor

The elementary principle of electromechanical energy conversion in a solenoid explains the torque production in the SRM. In Figure 5 (a), a solenoid with N turns is shown. A current i, excites the solenoid and a flux ϕ is produced. With an increase in the excitation current, the armature moves towards the fixed yoke under the effect of magnetomotive force produced by the excitation current [25].

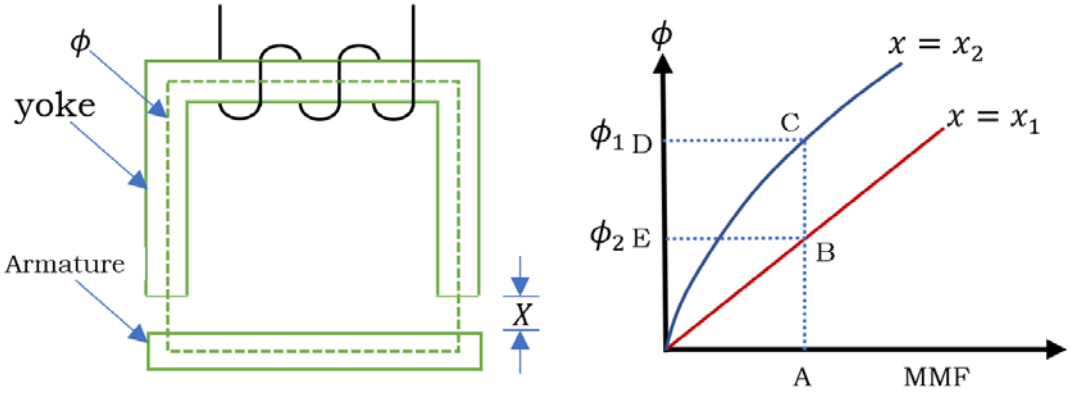

FIG 5. Solenoid and its characteristics. (a) A solenoid. (b) Flux v. mmf characteristics

Preprints (www.preprints.org) | NOT PEER-REVIEWED | Posted: 7 December 2022 doi:10.20944/preprints202212.0119.v1

Figure 5 (b) shows the plot between the flux and magnetomotive force (mmf) for two values of air gap, x_1 and x_2. The air gaps x_1 and x_2 are chosen such that, $x_1 > x_2$. The plot shows that the flux vs mmf characteristics are linear for x_1,and as the reluctance of the air gap is more prevalent making the flux lower in the magnetic circuit. The electrical input energy is given by [25]:

$$W_e = \int ei\, dt = \int i\, dt \frac{dN\phi}{dt} = \int Ni\, d\phi = \int F\, d\phi$$

where e is the induced emf and F is the mmf. This input electrical energy, W_e, is equal to the sum of energy stored in the coil, W_f , and energy converted into mechanical work W_m is written as

$$W_e = W_f + W_m$$

When the mechanical work done is zero, as in the case of the armature starting from position x_1, the stored field energy is equal to the input electrical energy. This accords to the area OBEO shown in Figure 5 (b). The complement of the field energy, is termed as coenergy, and is given by the area OBAO shown in Figure 5 (b) and can be exacted mathematically as $\int \phi\, dF$. Similarly, for the position x_2, of the armature, the field energy correlatess to area OCDO and the coenergy is given by area OCAO. For incremental changes,

$$\delta W_e = \delta W_f + \delta W_m$$

For a constant excitation of F1 given by the operating point A in Figure 5 (b), the various energies are derived as:

$$\delta W_e = \int_{\phi_1}^{\phi_2} F_1 d\phi = F_1(\phi_2 - \phi_1) = area(BCDEB)$$

$$\delta W_f = \delta W_{f|x=x_1} - \delta W_{f|x=x_2} = area(OCDO) - area(OBEO)$$

Then

$$\delta W_m = \delta W_e - \delta W_f = area(OBCO)$$

and this is the area constituted between the two curves for any given magnetomotive force. Considering the case of a rotating machine, the incremental mechanical energy expressed in terms of the electromagnetic torque and the change in rotor position is given by:

$$\delta W_n = T_e \delta\theta$$

where T_e is the electromagnetic torque and $\delta\theta$ is the incremental rotor angle. Thus, the electromagnetic torque is given by

$$T_e = \frac{\delta W_m}{\delta\theta}$$

When the condition of constant excitation (i.e., when the MMF is constant is considered), the incremental mechanical work done is the same as the rate of change of coenergy, which is nothing but the complement of the field energy. Hence, the incremental mechanical work done is expressed as [26]:

$$\delta W_m = \delta W_f'$$

Preprints (www.preprints.org) | NOT PEER-REVIEWED | Posted: 7 December 2022 doi:10.20944/preprints202212.0119.v1

$$W_f' = \int \phi \, dF = \int \phi \, d(Ni) = \int (N\phi) \, di = \int \lambda(\theta, i) di = \int L(\theta, i) i \, di$$

where the inductance, L, and flux linkages, λ, are functions of the rotor position and current. Considering two rotor positions, θ_2 and θ_1 the change in coenergy is occurred. Hence, the air gap torque in terms of the coenergy represented as a function of rotor position and current is given by

$$T_e = \frac{\delta W_m}{\delta \theta} = \frac{\delta W_f'}{\delta \theta} = \frac{\delta W_f'(i, \theta)}{\delta \theta}\Big|_{i=constant}$$

For a given current, if the inductance varies linearly with rotor position, which is found to be common, is not the case in practice, the torque can be derived as:

$$T_e = \frac{dL(\theta, i)}{d\theta} \frac{i^2}{2}$$

Where

$$\frac{dL(\theta, i)}{d\theta} = \frac{L(\theta_2, i) - L(\theta_1, i)}{\theta_2 - \theta_1}\Big|_{i=constant}$$

and this differential inductance can be considered to be the torque constant expressed in $N \cdot m/A^2$.

As seen in the above equations, the electromagnetic torque produced is proportional to the square of the current and so as to obtain a unidirectional torque, the current is to be unipolar. And, this unipolar current requirement paves to be advantageous in the requirement of power switch in the converter circuit. The output of the converter circuit is connected to the motor. Only one power switch is needed for the current control in phase winding [27] in SRM. With this feature, the number of power switches required in the converter circuit are reduced to a great extent. The result of reduced power switches in the converter leads the drive to be economical. The feature of torque produced is proportional to the square of the current resembles a dc series motor; and thus, the starting torque is high in SRM. A generating action is realized with unipolar current due to its operation on the negative slope of the inductance profile. For the generating action, the rotation can be reversed in direction by shifting the sequence of stator excitation, which is an uncomplicated operation. A controllable converter is required for SRM. It cannot be operated on a three-phase supply line directly. This attribute results in comparatively expensive motor drive than induction motor and synchronous motor, when employed for constant speed applications. The dependance on power converter makes it an inherently variable-speed motor drive system [28].

The control of current can precisely regulate the air gap torque. In many machines, such as in ac and dc machines, the airgap torque is directly proportional to the excitation current or a transformed current variable [29]. Thus, the controlling of the torque is direct in the machines. And, this results that the system now converts in to a linear torque amplifier such that the drive system now offers very high-speed performance in its speed control. The airgap torque and excitation current have a non-linear relationship in SRM. In SRM, three-dimensional relationship between the flux linkages, rotor position, and excitation current contributes to nonlinear three
dimensional relationships between the airgap torque, rotor position, and excitation current. The elicitation of the excitation current reference from the airgap torque reference is made adopting the three-dimensional relationship. Whereas, in all other motor drives,

Preprints (www.preprints.org) | NOT PEER-REVIEWED | Posted: 7 December 2022 doi:10.20944/preprints202212.0119.v1

two-dimensional relationship is used. Thus, it makes the controlling action is highly complex when making a linear torque amplifier [30].

The torque control methods are reliant on the number of phases that are excited at a given instant of time and the current control efficacy of the system. For example, consider a single phase excitation control method. Here, only one phase winding is energized at a given instant of time. During the commutation of one phase and initiation of another phase, the current flows in two phases. If the current is not controlled in the outgoing phase and only controlled in the incoming phase, the sum of the airgap torques contributed by the outgoing and incoming phases during this interval need not be a constant. The resultant torque normally has a trough during this interval which is known as commutation interval. During this commutation interval, the torque ripple increases. Torque ripple is unwelcome in a high-performance drive system as it may lead to a speedier ripple and greater machine losses [31].

3. Torque Ripple Minimization Techniques:

Two minimization techniques are approaches are there in minimization of torque ripples [32].
. Machine Design Improvement
. Control Strategy Improvement

3.1. Torque Ripple Minimization through Machine Design:

By revising the stator and rotor pole geometry torque ripple is reduced in SRM through the machine design and magnetic design with design steps is explained in [33] by undertaking the torque ripple and acoustic noise that could be generated in design process. With the help of mathematical equations, the stator and rotor poles geometry, the machine specification (torque, speed, noise level, etc.) are determined. The parameters which effect the torque ripple are stator arc, Bs, rotor arc, ß, are determined for machine design. To minimize the torque ripple and noise generated, magnetic behavior can be determined using Finite Element Analysis (FFA) tools and in [34] design which includes skewing the rotor poles is presented. The main purpose of rotor construction is to weaken torque ripple while maintaining high torque density. With this design no development was there in terms of torque density but shows development in torque ripple coefficient and drawback is that it could conclude in attrition of the maximum torque achieved due to increased effective airgap through the new geometric design of the rotor/stator poles.

3.2. Torque Ripple Minimization through Control Strategy Improvements

A. Current Profiling

Current profiling is the shaping of the current. The torque produced is a function of instantaneous value of current and the inductance. Thus, current profiling can present a control on the torque ripple. Profiling the phase currents leads to the shaping of the current and thus minimize torque ripple.
Extraction of the excitation current reference from the airgap torque reference is contrived using the three-dimensional relationship. Many literatures proposed various current profiling methods. The proposed methods in these literatures usually differ in the control algorithm employed in the implementation [35]. The chief concept of current profiling is to enumerate the shape of current through an off-line method to reach zero torque ripple and then the controller is modeled to follow the generated current profile [36]. Current profiling implements the values of three currents taken from the lookup table of $I = f(T, \theta)$ which is enumerated for rising current and falling current. When enumerating the current profile, necessarily the torque characteristic is transformed from $T = f(I, \theta)$ to $I = f(T, \theta)$. An initial condition is conceived from the $T = f(I, \theta)$ lookup table before the current profile is fine tuned.
Different methods are available in specifying the initial current profile. Current profile is enumerated through FEA simulation. This gives the initial current profile as presented in [37,38]. And then it is finely tuned with the torque feedback. The final current profile is generated after several iterations. The number of iterations depending on the torque ripple requirement. While in [39], an

Preprints (www.preprints.org) | NOT PEER-REVIEWED | Posted: 7 December 2022 doi:10.20944/preprints202212.0119.v1

imperceptibly different approach is presented where mathematical equation to enumerate the maximum and minimum currents is derived. Based on the rotor position step and machine current specification, the current profile is then generated. The max and min current are derived as follows [40]:

$$i_{max}(\theta_k) = i(\theta_{k-1}) + \frac{1}{L\left(i(\theta_{k-1}, \theta_{k-1})\right)}\left(v - iR(\theta_{k-1}) - \frac{dL(i(\theta_{k-1}), \theta_{k-1})}{d\theta}\omega i(\theta_{k-1})\right)dt$$

$$i_{min}(\theta_k) = i(\theta_{k-1}) + \frac{1}{L\left(i(\theta_{k-1}, \theta_{k-1})\right)}\left(-v - iR(\theta_{k-1}) - \frac{dL(i(\theta_{k-1}), \theta_{k-1})}{d\theta}\omega i(\theta_{k-1})\right)dt$$

The new current profile boundaries are determined as i_{max} and i_{min}. The relationship of $I = f(T, \theta)$ is then computed using a current profiling control algorithm. The torque ripple is found to curtailed up to 18 % by the current profiling method [41].

Torque Sharing Function:

Torque sharing function is important for the current profiling method as it involved single shaping and generally used in torque ripple minimization technique. Torque is shaped by continues measure the position of the rotor angle [42]. To meet the primary objective of low torque ripple, TSFs is provided for ideal torque sharing between individual phases. TSFs are based on linear, sinusoidal, exponential curves and cubic which used usually and TSF curves used to express the TSF which specifies the SRM and the torque ripple necessity [43].

A torque sharing function (TSF) intelligently divides a constant torque reference between the particular phases by defining a reference current profile for each phase. Ideally, when this current reference profile is tracked by a current controller, the total torque contribution from all of the phases will add up to the constant torque, thus eliminating torque ripple. A very simple way of defining a torque sharing function is through using analytical expressions to model the dynamic behavior of the phase torque contribution [44].

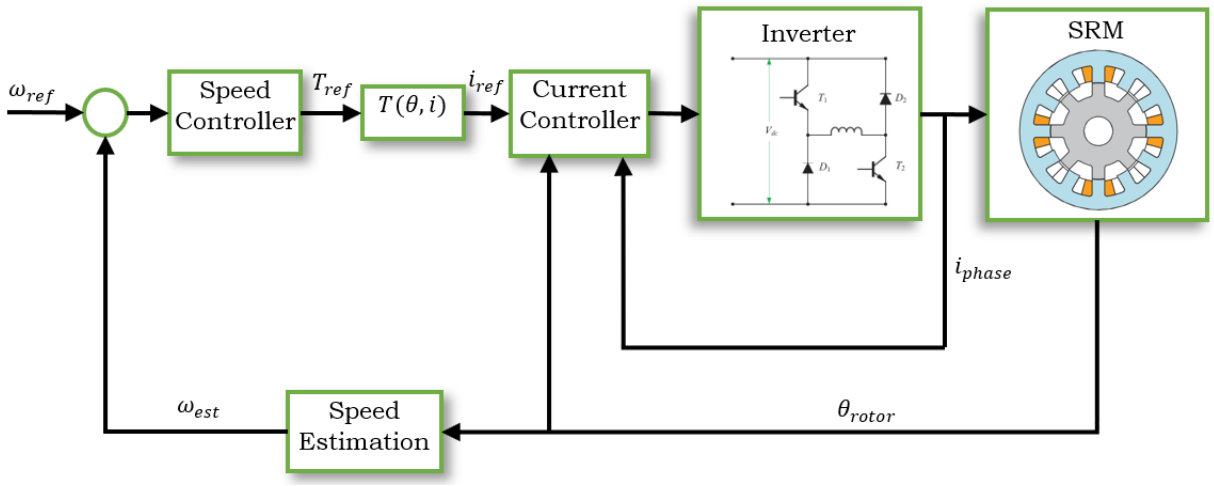

Fig 6. Overview of control structure for SRM with TSF.

the torque reference of the i[th] phase is defined as [45]

$$T_{ref}(i) = \begin{cases} 0 & 0 \le \theta < \theta_{ON} \\ T_{ref} f_{rise}(\theta) & \theta_{ON} \le \theta < \theta_{ON} + \theta_{OV} \\ T_{ref} & \theta_{ON} + \theta_{OV} \le \theta < \theta_{OFF} \\ T_{ref} f_{fall}(\theta) & \theta_{OFF} \le \theta < \theta_{OFF} + \theta_{OV} \\ 0 & \theta_{OFF} + \theta_{OV} \le \theta < \theta_p \end{cases}$$

Preprints (www.preprints.org) | NOT PEER-REVIEWED | Posted: 7 December 2022 doi:10.20944/preprints202212.0119.v1

where $T_{ref}(i)$ is the reference torque for ith phase, T_{ref} is total torque reference, $f_{rise}(\theta)$ is the rising function for the incoming phase that increases from zero to one, and $f_{fall}(\theta)$ is the decreasing function for the outgoing phase that decreases from one to zero, for some rotor position, θ

B. Direct Instantaneous Torque Control:

Direct Instantaneous Torque Control (DITC) is the method which has torque ripple minimization control to avoid use of high precision rotor position sensor and it is proposed in 2003. In DITC, current or torque profiles and commutating waveforms are not used and the 1nstantaneous torque vales is measured from the SMR terminal. It needs a precise elaborate model to direct phase current as a function of torque and rotor position [46].

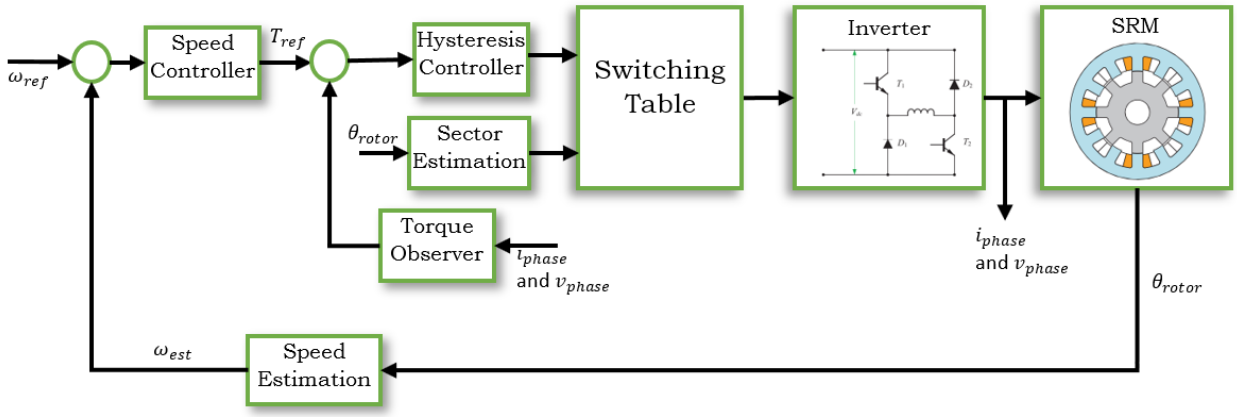

Fig 7. DITC control system block diagram

The torque $T(\theta, i)$ is depends on current and rotor position and to figure correct torque computation and for precise control to be accomplished, accurate continuous rotor position measurement is desired. The torque characteristic is a function of flux linkage instead of rotor position $T(\lambda, i)$ which is avoided. A look-up table is made to calculate the total torque T_{tot}. All activated machine phase is generated by switching signals as well as a digital torque hysteresis controller [47]. Hysteresis controller use to get high bandwidth of switching signals and it needs the broad range of operations. The torque pulsations which subsidize to torque ripple is condensed using DITC and switching strategy plays main role in minimizing the torque ripple. 1y simulation, the torque ripple reduces to 38% of the machine average torque of 40Nm. In DITC no torque sharing function is desired and direct control of instantaneous torque where no profiling is needed and it offers simple control structure with torque ripple minimization [48].

The torque $T(\theta, i)$ is depends on current and rotor position and to figure correct torque estimation and for precise control to be executed, accurate continuous rotor position measurement is desired. The torque characteristic is a function of flux linkage instead of rotor position $T(\lambda, i)$ which is avoided. A look-up table is made to calculate the total torque T_{tot}. All activated machine phase is generated by switching signals as well as a digital torque hysteresis controller [47]. Hysteresis controller use to get high bandwidth of switching signals and it needs the broad range of operations. The torque pulsations which subsidize to torque ripple is condensed using DITC and switching strategy plays main role in minimizing the torque ripple. By simulation, the torque ripple reduces to 38% of the machine average torque of 40Nm. In DITC no torque sharing function is desired and direct control of instantaneous torque where no profiling is needed and it offers simple control structure with torque ripple minimization [48].

4. Review of Previous Work

In [49] The non-dominated sorting genetic algorithm (NSGA-11) for SRM optimization is presented and air gap length is suggested design for the SMR. Maximum efficiency, maximum average torque and minimal iron weight are implemented in multi-objective design. Finite element analysis (FEA) is used to get values in the optimization process and 8/6, 6/4 SRM designs are implemented. Design parameters improves average torque and effectiveness with reduced iron weight.

 doi:10.20944/preprints202212.0119.v1

In [50] Multi-objective Jaya method is used to optimize SRM design in which greater degree of variety, as seen by the findings and 8/6,6/4 were optimized using the Mo-JAYA algorithm. The Mo-JAYA results are compared to the non-dominated sorting genetic algorithm (NSGA-11). FEMM4.2 software is used in optimization program in the Lua programming language.

In [51] To optimize the structural design of a 12/8 switching reluctance motor are used by single objective genetic algorithms. Optimize output torque by narrowing each of the four tooth roots, widening each of the four tooth tips and increasing the stator outer diameter are the main goal of this optimization is to optimize output torque. Here small electric car uses a 12/8 switching reluctance motor and the finite elements are used to assess motor model. Enhanced motor delivers a 25% rise in average torque over the original design.

In [52] To find the finest motor design parameters for the ISRM, an ant colony optimization approach was employed. By setting the optimize issue in the dimensions of a motor in order to optimize torque and effectiveness. MATLAB software is used in analytical models to determine torque and efficiency figures, taking into consideration the motors non-linearity.

In [53] In this work an appropriate nonlinear torque model that is recursively resistant square support vector regression (RR-LSSVR). Segmented motor is modelled with SR motor in the (SSRM) and the features are non-linear qualities in magnetic and torque. It is proved that an accurate inductance measuring technique and a torque calculation procedure and it is fast and accurate this particular algorithm. When compared to other models, the RR-LSSVR alter weights based on mistakes are clarified and recommended models' correctness in real-world settings that were created on 16/ 10 SSRM.

In [54] An electric vehicle (EV) switching reluctance motor (SRM) use a three-phase 12/8 Grey Wolf Optimizer (GWO) is optimized and SRM output torque density is enhanced. By using the FEM approach analysis of the suggested motors properties and optimization procedure were conducted. In optimization constraints the current density, optimization procedure, the maximum flux density and other motor volume are detailed. To get the optimal value, optimized values are directed to FEM software for analysis each repetition. In this, working prototype motor built and its presentation may be verified empirically. A rise in torque of 120 % may be attained by retaining the method, contempt the same volume.

In [55] Two types of uncertainty like variation outer disorder and the model error are in traditional H-infinity control which has an external control method. The H-infinity control mechanism is a closed loop controller, decisive the ideal control weight is difficult. The ideal weight for the transfer function matrix is suggested control process by an effective optimization tool and Genetic algorithm (GA) is used. By this technique, the SRMS speed is adjusted using MATLABS built-in toolset and in each interval the weight noise setting is resolute. H-infinity optimum control use GA method to get the ideal weight noise setting.

In [56] This research provides a unique multi objective optimization design technique for a switching reluctance motor (SRM) for low-speed electric cars and the design parameters for SRM are acceleration time, maximum speed, maximum climbing gradient, torque ripple factor, and energy usage ratio to optimized the SRMs performance. By using the MATLAB/Simulink, the SRMS finite element model and the vehicle balance equation, a dynamic simulation model for a low-speed pure EV propulsion system was created. The geometric parameters of the SRM are then optimized for many objectives by using Taguchi-Chicken swarm optimization technique.

In [57] For variable speed operation, the switching reluctance motor (SRMs) are extremely endorsed option. The linear quadratic regulator with integral action (LOI) technique is used in resilient and simple to change while utilizing plants in state spaces and manual adjustment of Q and R matrix weightings is provided by LQR systems and allowing the user to get desired of expertise in the field and assessment is done among metaheuristic algorithms for designing the LQI controller as well as PID controllers to identify the optimal approach for LQI controller design modification of Q and R variables in SR motors. In this work, the LQI parameters are weighted in an optimal manner and gains in controller may regulate frequently, making the hybrid controller (LQI+GA) more influential in multivariable system's control.

In [58] The hybrid electric vehicles (HEVs) are cost-effective to increase the vehicle's reliability and lower its fuel usage by using the belt-driven starter/generator (BSG) and decrease CO2 emission to 10%. Motor and generator are served by the core of the BGS

 doi:10.20944/preprints202212.0119.v1

system in an electrical unit and proved the novel multimode optimization technique for switching reluctance machines in order to optimize the motor and generator simultaneously. The multi objective optimization takes seven different design factors and four different driving modes. Sum of techniques is used to rise the efficiency of multimode optimization. The Kriging model is used to approximate the FEM throughout the optimization process and optimum designs increase the SSRMS presentation in all operating conditions.

Method	**Implemented Process**	**Merits**	**Demerits**	**Ref**
SPAM (Angle Modulation)	Finding switch on and off angles, determine required current magnitude and phase angles	Better efficiency, improved torque/speed ratio, reduced ripples in the torque	Controlling torque and current mutually is no possible, storage of huge current data increases the cost	59
DTC and ATC	Estimation of torque during speed control and torque control using hysteresis bands	Rapid torque control by DTC, torque ripple minimization to IEEE standards	Parameters of the machine should be known	60
Torque sharing function-based method	Torque sharing function, generating current refence using torque control, using hysteresis band to track reference current	Easily controlled torque, determined torque waveforms, smooth torque over a wide speed range	Need i-T-θ characteristics, offline desired torque waveforms	61
Feedback linearization control	Transform the nonlinear system into a linear model	Reduced torque ripple, no nonlinear terms in feedback loop, provide required decoupling among currents	Not adapt the change of uncertain parameters, complex algorithm	62
Iterative learning controller	Add a compensation current to the phase current reference for current tracking	No need to identify the system parameters, achieve perfect current tracking under different operation conditions	Degraded performance to transients, restriction of iteration cycle	63
Intelligent control	Used for offline or online optimization of phase currents	Strong self learning, adaptive ability, reduced torque ripple, no rely on machine parametrs,	Complex computational algorithm	64
Share switched converters	Shared switch asymmetric half-bridge converters,	Minimization of the number of power devices,	Fault-tolerance will be reduced, the current stress in the common switch and diode is higher	65
Split converters	Method of compensating midpoint voltage	the performance of the motor is increased with the reduction of the	the effect of the floating of the midpoint voltage and poor fault tolerance	66

 doi:10.20944/preprints202212.0119.v1

		fluctuation of midpoint voltage.		
C-dump converters	C-dump converter with inductor	demagnetize faster during the phase replacement process, energy after being discharged to the capacitor, directly used into the next phase and not returned to the DC source	need for an extra capacitor and the current stress of switches is high	67
FS-PTC	improved constrained-state perceptive torque controls	limit the torque swell of traded reluctance motor (SRM) drive	influences the capability of the drive. The total drive capability is diminished by 4–9%	68

Direct instantaneous torque control (DITC) based on torque sharing function (TSF) also known as TSF-DITC is currently one of the main methods to suppress the torque ripple of SRM. In this method, TSF are used to distribute the total torque to individual phase, and then the phase torque hysteresis drives the motor according to appropriate control rules. A multi-level converter is presented in the reference [69]. Based on TSF-DITC a multi-level converter is selected and different control rules are selected for different conduction regions. This accelerates the excitation and demagnetization of the commutation region and thus, fast torque tracking is achieved. Reference [70] proposes a direct instantaneous torque control method for SRM based on the optimal angle adaptive TSF. Reference [71] uses the dynamic shapeless TSF to improve the system efficiency in SRM torque control. The system performance is influenced to a great extent by different commutation points. In short, although the TSF-DITC algorithm is simple, easy to implement and has a certain degree of torque ripple suppression effect, it is necessary to formulate complex hysteresis control rules in the commutation region, and it is difficult to optimize multiple performance indexes at the same time. Torque ripple reduction is possible by optimizing hysteresis bandwidth with respect to torque error using any population based naturally inspired optimization algorithms.

5. Conclusion

For commercial utilization of SRM torque ripple is the major drawback. Torque ripple which outcomes in increased trembling and noise may not be a feasible characteristic of the SRM for industrial applications. As such lessening torque ripple in the SRM is important for SRM working in commercial applications. Torque ripple can be lessened by refining the machine design as proposed in this literature. Withal, torque ripple curtailment by machine design deviations, rises the mechanical complexity which increases production cost and reduces the maximum possible torque. Torque ripple reduction by control approach delivers a more economical and optimal in dealing with torque ripple. Many control approaches presented for torque ripple redu 1 ion has been studied and revised in this paper. Every proposed approach offers enhancement in torque ripple generated by the SRM. In spite of the amount of effort finished in minimizing the torque ripple, there are still extents of the SRM working where the torque ripple has not been well considered yet. Several practical features of modeling, design, analysis and control in switched reluctance machines have been revised comprehensively. Regardless of good scientific progress in switched reluctance machines, there appears to be an ex 151sive gap when aspiring to the industrial applications. The current trends in research strives to fill this void by the establishment of standards and the development of cost-effective controllers applicable in motion control systems.

References

1. Lopez, Gabriel Gallegos. *Sensorless control for switched reluctance motor drives*. University of Glasgow (United Kingdom), 1998.
2. Sirimanna, Samith, et al. "Comparison of electrified aircraft propulsion drive systems with different electric motor topologies." *Journal of Propulsion and Power* 37.5 (2021): 733-747.
3. Mvungi, Nerey H. "Sensorless commutation control of switched reluctance motor." *World Academy of Science, Engineering and Technology* 25 (2007): 325-330.
4. Donaghy-Spargo, C. M. "Synchronous reluctance motor technology: opportunities, challenges and future direction." *Engineering & technology reference.* (2016): 1-15.
5. Mitra, Rakesh, and Yilmaz Sozer. "Torque ripple minimization of switched reluctance motors through speed signal processing." *2014 IEEE Energy Conversion Congress and Exposition (ECCE)*. IEEE, 2014.
6. Tseng, K. J., and Shuyu Cao. "A SRM variable speed drive with torque ripple minimization control." *APEC 2001. Sixteenth Annual IEEE Applied Power Electronics Conference and Exposition (Cat. No. 01CH37181)*. Vol. 2. IEEE, 2001.
7. Chuang, Tzu-Shien. "Acoustic noise reduction of a 6/4 SRM drive based on third harmonic real power cancellation and mutual coupling flux enhancement." *Energy Conversion and Management* 51.3 (2010): 546-552.
8. Chai, J. Y., Y. W. Lin, and C. M. Liaw. "Comparative study of switching controls in vibration and acoustic noise reductions for switched reluctance motor." *IEE Proceedings-Electric Power Applications* 153.3 (2006): 348-360.
9. Kazemi, A. R., et al. "A novel sensorless method for rotor position detection in bifilar SRM drive." *2010 IEEE International Conference on Power and Energy*. IEEE, 2010.
10. Zhang, Man, et al. "Improvement of the variable turn-off angle control for SRM regarding vibration reduction." *2017 IEEE International Electric Machines and Drives Conference (IEMDC)*. IEEE, 2017.
11. Ding, Wen, et al. "Design consideration and evaluation of a 12/8 high-torque modular-stator hybrid excitation switched reluctance machine for EV applications." *IEEE Transactions on industrial electronics* 64.12 (2017): 9221-9232.
12. Mousavi-Aghdam, Seyed Reza, et al. "Design and analysis of a novel high-torque stator-segmented SRM." *IEEE Transactions on Industrial Electronics* 63.3 (2015): 1458-1466.
13. Asgar, Majid, Ebrahim Afjei, and Hossein Torkaman. "A new strategy for design and analysis of a double-stator switched reluctance motor: Electromagnetics, FEM, and experiment." *IEEE Transactions on Magnetics* 51.12 (2015): 1-8.
14. Li, G. J., et al. "Comparative study of switched reluctance motors performances for two current distributions and excitation modes." *2009 35th Annual Conference of IEEE Industrial Electronics*. IEEE, 2009.
15. Ma, X. Y., et al. "Recent development of reluctance machines with different winding configurations, excitation methods, and machine structures." *CES Transactions on Electrical Machines and Systems* 2.1 (2018): 82-92.
16. Ma, X. Y., et al. "Quantitative analysis of contribution of air-gap field harmonics to torque production in three-phase 12-slot/8-pole doubly salient synchronous reluctance machines." *IEEE Transactions on Magnetics* 54.9 (2018): 1-11.
17. Burress, Tim, and Curt Ayers. "Development and experimental characterization of a multiple isolated flux path reluctance machine." *2012 IEEE Energy Conversion Congress and Exposition (ECCE)*. IEEE, 2012.
18. Andrada Gascón, Pedro. "SRM drives an alternative for E-traction: Presentation of the workshop." *Workshop SRM Drives an Alternative for E-Traction: Proceedings: February 2, 2018, EPSEVG-UPC Vilanova i la Geltrú (Barcelona) Spain*. Universitat Politècnica de Catalunya. GAECE-Grup d'Accionaments Elèctrics amb Commutació Electrònica, 2018.
19. Kabir, Md Ashfanoor, and Iqbal Husain. "Design of mutually coupled switched reluctance motors (MCSRMs) for extended speed applications using 3-phase standard inverters." *IEEE Transactions on Energy Conversion* 31.2 (2015): 436-445.
20. Li, G. J., et al. "Comparative studies of torque performance improvement for different doubly salient synchronous reluctance machines by current harmonic injection." *IEEE Transactions on Energy Conversion* 34.2 (2018): 1094-1104.

 doi:10.20944/preprints202212.0119.v1

21. Azer, Peter, Berker Bilgin, and Ali Emadi. "Comprehensive analysis and optimized control of torque ripple and power factor in a three-phase mutually coupled switched reluctance motor with sinusoidal current excitation." *IEEE Transactions on Power Electronics* 36.6 (2020): 7150-7164.
22. Ma, Xiyun, et al. "Investigation on synchronous reluctance machines with different rotor topologies and winding configurations." *IET Electric Power Applications* 12.1 (2018): 45-53.
23. Dong, Jianning, et al. "Advanced dynamic modeling of three-phase mutually coupled switched reluctance machine." *IEEE Transactions on Energy Conversion* 33.1 (2017): 146-154.
24. Reddy, Battu Prakash, Prathap Reddy Bhimireddy, and Sivakumar Keerthipati. "A sense winding system and dynamic current profiling to reduce torque ripple of SRM." *International Transactions on Electrical Energy Systems* 30.2 (2020): e12261.
25. Meng, Bin, et al. "Novel magnetic circuit topology of linear force motor for high energy utilization of permanent magnet: Analytical modelling and experiment." *Actuators*. Vol. 10. No. 2. MDPI, 2021.
26. Ling, Xiao, et al. "Precise in-situ characterization and cross-validation of the electromagnetic properties of a switched reluctance motor." *Artificial Intelligence in Agriculture* 4 (2020): 74-80.
27. Sovicka, Pavel, Pavol Rafajdus, and Vladimir Vavrus. "Switched reluctance motor drive with low-speed performance improvement." *Electrical Engineering* 102.1 (2020): 27-41.
28. Riyadi, Slamet. "A control strategy for SRM drive to produce higher torque and reduce switching losses." *Journal of Electrical Systems* 14.4 (2018): 205-216.
29. Khan, Yawer Abbas, and Vimlesh Verma. "Novel speed estimation technique for vector-controlled switched reluctance motor drive." *IET Electric Power Applications* 13.8 (2019): 1193-1203.
30. Ma, Mingyao, et al. "A switched reluctance motor torque ripple reduction strategy with deadbeat current control." *2019 14th IEEE Conference on Industrial Electronics and Applications (ICIEA)*. IEEE, 2019.
31. Kumagai, Takahiro, Jun-ichi Itoh, and Keisuke Kusaka. "Reduction method of torque ripple, dc current ripple, and radial force ripple with control flexibility of five-phase srm." *2020 IEEE Energy Conversion Congress and Exposition (ECCE)*. IEEE, 2020.
32. Moradi CheshmehBeigi, Hassan, and Alireza Mohamadi. "Torque ripple minimization in SRM based on advanced torque sharing function modified by genetic algorithm combined with fuzzy PSO." *International Journal of Industrial Electronics Control and Optimization* 1.1 (2018): 71-80.
33. Lee, Jin Woo, et al. "New rotor shape design for minimum torque ripple of SRM using FEM." *IEEE transactions on magnetics* 40.2 (2004): 754-757.
34. Kabir, Md Ashfanoor, and Iqbal Husain. "Segmented rotor design of concentrated wound switched reluctance motor (SRM) for torque ripple minimization." *2016 IEEE Energy Conversion Congress and Exposition (ECCE)*. IEEE, 2016.
35. Dúbravka, Peter, et al. "Control of switched reluctance motor by current profiling under normal and open phase operating condition." *IET Electric Power Applications* 11.4 (2017): 548-556.
36. Khalili, H., E. Afjei, and A. Najafi. "Torque ripple minimization in SRM drives using phase/current profiles." *2007 International Aegean Conference on Electrical Machines and Power Electronics*. IEEE, 2007.
37. Mitra, Rakesh, et al. "Torque ripple minimization of switched reluctance motors using speed signal based phase current profiling." *2013 IEEE Energytech*. IEEE, 2013.
38. Saidani, Sihem, Mohamed Radhouan Hachicha, and Moez Ghariani. "A New Phase Current Profiling with FLC for Torque Optimization of 12/8 SRM." *International Journal of Electrical & Computer Engineering (2088-8708)* 6.5 (2016).

 doi:10.20944/preprints202212.0119.v1

39. Mikail, Rajib, et al. "Four-quadrant torque ripple minimization of switched reluctance machine through current profiling with mitigation of rotor eccentricity problem and sensor errors." *IEEE Transactions on Industry Applications* 51.3 (2014): 2097-2104.
40. Huang, Liren, et al. "Novel current profile of switched reluctance machines for torque density enhancement in low-speed applications." *IEEE Transactions on industrial electronics* 67.11 (2019): 9623-9634.
41. Makino, H., et al. "Instantaneous current profiling control for minimizing torque ripple in switched reluctance servo motor." *2015 IEEE Energy Conversion Congress and Exposition (ECCE)*. IEEE, 2015.
42. Xue, X. D., Ka Wai Eric Cheng, and Siu Lau Ho. "A control scheme of torque ripple minimization for SRM drives based on flux linkage controller and torque sharing function." *2006 2nd international conference on power electronics systems and applications*. IEEE, 2006.
43. Chithrabhanu, Arun, and Krishna Vasudevan. "Online compensation for torque ripple reduction in SRM drives." *2017 IEEE Transportation Electrification Conference (ITEC-India)*. IEEE, 2017.
44. Li, Haoding, Berker Bilgin, and Ali Emadi. "An improved torque sharing function for torque ripple reduction in switched reluctance machines." *IEEE Transactions on Power Electronics* 34.2 (2018): 1635-1644.
45. Xia, Zekun, et al. "A new torque sharing function method for switched reluctance machines with lower current tracking error." *IEEE Transactions on Industrial Electronics* 68.11 (2020): 10612-10622.
46. Sun, Jianzhong, et al. "Simulation of the direct instantaneous torque control of SRM using MATLAB." *International Conference on Automatic Control and Artificial Intelligence (ACAI 2012)*. IET, 2012.
47. Xu, Aide, et al. "A new control method based on DTC and MPC to reduce torque ripple in SRM." *IEEE Access* 7 (2019): 68584-68593.
48. Veena, Nayak D., and Naik L. Raghuram. "Minimization of torque ripple using DITC with optimum bandwidth and switching frequency for SRM employed in electric vehicle." *2017 International Conference on Smart grids, Power and Advanced Control Engineering (ICSPACE)*. IEEE, 2017.
49. El-Nemr, Mohamed, et al. "Finite element based overall optimization of switched reluctance motor using multi-objective genetic algorithm (NSGA-II)." *Mathematics* 9.5 (2021): 576.
50. Afifi, Mohamed, et al. "Multi-Objective Optimization of Switched Reluctance Machine Design Using Jaya Algorithm (MO-Jaya)." *Mathematics* 9.10 (2021): 1107.
51. Sholahuddin, Umar, Agus Purwadi, and Yanuarsyah Haroen. "Structural Optimizations of a 12/8 Switched Reluctance Motor using a Genetic Algorithm." *International Journal of Sustainable Transportation Technology* 1.1 (2018): 30-34.
52. YILDIZ, Ahmet, Mehmet POLAT, and Mahmut Temel Özdemir. "Design optimization of inverted switched reluctance motor using ant colony optimization algorithm." *2018 International Conference on Artificial Intelligence and Data Processing (IDAP)*. IEEE, 2018.
53. Wu, Jiangling, Xiaodong Sun, and Jianguo Zhu. "Accurate torque modeling with PSO-based recursive robust LSSVR for a segmented-rotor switched reluctance motor." *CES Transactions on Electrical Machines and Systems* 4.2 (2020): 96-104.
54. Vuddanti, Sandeep, Vinod Karknalli, and Surender Reddy Salkuti. "Design and comparative analysis of three phase, four phase and six phase switched reluctance motor topologies for electrical vehicle propulsion." *Bulletin of Electrical Engineering and Informatics* 10.3 (2021): 1495-1504.
55. Rigatos, Gerasimos, Pierluigi Siano, and Sul Ademi. "Nonlinear H-infinity control for switched reluctance machines." *Nonlinear Engineering* 9.1 (2020): 14-27.
56. Hajiabadi, Hojjat, Mohsen Farshad, and MohammadAli Shamsinejad. "Multi-objective optimization and online control of switched reluctance generator for wind power application." *International Journal of Industrial Electronics Control and Optimization* 4.1 (2021): 33-45.

57. Souza, Darielson A., et al. "Optimal lqi and pid synthesis for speed control of switched reluctance motor using metaheuristic techniques." *International Journal of Control, Automation and Systems* 19.1 (2021): 221-229.
58. Bai, Shengxi, and Chunhua Liu. "Overview of energy harvesting and emission reduction technologies in hybrid electric vehicles." *Renewable and Sustainable Energy Reviews* 147 (2021): 111188.
59. Gundogmus, Omer, et al. "Current profile optimization method for simultaneous dc-link current ripple and acoustic noise minimization in switched reluctance machines." *2020 IEEE Energy Conversion Congress and Exposition (ECCE)*. IEEE, 2020.
60. Sun, Xiaodong, et al. "Direct torque control based on a fast modeling method for a segmented-rotor switched reluctance motor in HEV application." *IEEE Journal of Emerging and Selected Topics in Power Electronics* 9.1 (2019): 232-241.
61. Üstün, Oğuz, and Mithat Önder. "An improved torque sharing function to minimize torque ripple and increase average torque for switched reluctance motor drives." *Electric Power Components and Systems* 48.6-7 (2020): 667-681.
62. Bober, Peter, and Želmíra Ferková. "Comparison of an off-line optimized firing angle modulation and torque sharing functions for switched reluctance motor control." *Energies* 13.10 (2020): 2435.
63. Shao, Zhen, and Zhengrong Xiang. "Adaptive iterative learning control for switched nonlinear continuous-time systems." *International Journal of Systems Science* 50.5 (2019): 1028-1038.
64. Kumar, R. Senthil, et al. "Intelligent Fuzzy controller based NT control of 5Φ SRM." *Materials Today: Proceedings* (2021).
65. Hu, Yanfang, Tao Wang, and Wen Ding. "Performance evaluation on a novel power converter with minimum number of switches for a six-phase switched reluctance motor." *IEEE Transactions on Industrial Electronics* 66.3 (2018): 1693-1702.
66. Y. Hu, C. Gan, W. Cao, C. Li and S. J. Finney, "Split Converter-Fed SRM Drive for Flexible Charging in EV/HEV Applications," in *IEEE Transactions on Industrial Electronics*, vol. 62, no. 10, pp. 6085-6095, Oct. 2015, doi: 10.1109/TIE.2015.2426142.
67. Setiawan, Kho Lukas Budi. "Analysis Performance of Capacitor Voltage in C-Dump Converter for SRM Drive." *2018 IEEE Student Conference on Research and Development (SCOReD)*. IEEE, 2018.
68. Li, Cunhe, et al. "An improved finite-state predictive torque control for switched reluctance motor drive." *IET Electric Power Applications* 12.1 (2018): 144-151.
69. Yang, Yang, et al. "Torque Compensation Method of Switched Reluctance Motor Adopting MPC Based on TSF-DITC." *Progress In Electromagnetics Research M* 110 (2022): 211-221.
70. Ren, Ping, et al. "Minimization of torque ripple in switched reluctance motor based on MPC and TSF." *IEEJ Transactions on Electrical and Electronic Engineering* 16.11 (2021): 1535-1543.
71. Sun, Xiaodong, et al. "Torque ripple reduction of SRM drive using improved direct torque control with sliding mode controller and observer." *IEEE Transactions on Industrial Electronics* 68.10 (2020): 9334-9345.